Cloud Publications
International Journal of Advanced Remote Sensing and GIS
2020, Volume 9, Issue 1, pp. 3289-3311
ISSN 2320 – 0243, Crossref: 10.23953/cloud.ijarsg.460

Research Article

Identification of Groundwater Potential Zones Using Analytical Hierarchy Process (AHP) and GIS-Remote Sensing Integration, the Case of Golina River Basin, Northern Ethiopia

Hindeya Gebru[1, 2], Tesfamichael Gebreyohannes[2], and Ermias Hagos[2]

[1]Department of Earth Sciences, Samara University, Samara, Ethiopia
[2]School of Earth Sciences, Mekelle University, Mekelle, Ethiopia

Correspondence should be addressed to Hindeya Gebru, *hindualem@gmail.com*

Publication Date: 6 May 2020

DOI: https://doi.org/10.23953/cloud.ijarsg.460

Abstract Groundwater is the main source of water both for domestic and irrigation purposes in the study area, Golina basin. The Golina basin is located in the North Wollo Administration, Amhara regional state, Northern Ethiopia. The study area has a surface area of 916.77 km^2 and is a semi-arid environment with an annual mean precipitation of 913 mm/year. Because of its presumed groundwater potential, the area has recently received significant attention from the regional and federal governments as well as investors. As a result, 81wells have been drilled for groundwater extraction mainly for irrigation purposes. About 182 springs and hand-dug wells have been developed for domestic purposes. However, little has been done to know the overall groundwater potential, the groundwater potential zonation and the sustainability of the current and planned groundwater extraction in the basin. Thus, the main objective of this work is to delineate groundwater potential zones of the area using an integrated method of AHP, GIS, and Remote sensing. A total of 10 thematic layers are used for the groundwater potential zone assessment. Based on the AHP method, the priority of the thematic layers with their weight are as follows: geology (0.22), geomorphologic landform (0.22), lineament density (0.17), slope (0.12), drainage density (0.09), soil (0.07), land use land cover (0.04), precipitation (0.04), normalized difference vegetation index (NDVI) (0.02) and topographic wetness index (TWI) (0.02). The groundwater potential zones of the area are computed using raster calculator in spatial analyst tool in GIS software and divided into five classes as very poor, poor, moderate, good and very good with area coverage of 93 km^2 (10%), 265km^2 (29%), 175 km^2(19%), 221 km^2(24%) and 162 km^2(18%) of the total area, respectively. The result is validated using the existing spring, hand-dug wells and borehole yields. Accordingly, the high yield boreholes are drilled and concentrated in very good groundwater potential zones whereas the low yield springs are developed in the very poor. Out of 263 water points 74, 72, 48, 59 and 10 water points are located in very good, good, moderated, poor and very poor groundwater potential zones, respectively. Mainly the very good groundwater potential fall in the alluvial deposit, plain and valley landforms, very low slope (flat), high lineament density, low drainage density, coarse soil textures, and water body and cultivated lands with high precipitation, NDVI and TWI. The result of this study can be used for the planning of new groundwater-based projects and the expansion of the existing irrigation project in the basin.

Keywords *Analytical Hierarchy Process; geographic information system; remote sensing; groundwater potential; Golina River Basin*

1. Introduction

1.1. General

Globally, groundwater is the source of one-third of all freshwater withdrawals (Taylor et al., 2013). It is a crucial natural resource for any economic development in arid and semi-arid countries that have a scarcity in their water resources (Kuisi et al., 2014). All development activities are directly and indirectly depend on groundwater resources. However, this resource is highly affected by existing geology, degree of chemical weathering, quality of recharge, level of groundwater, some surface element sources, etc. whereas surface water is normally affected by surface pollutants (Kaur et al., 2017). Naturally, surface water has less mineral content as compared to groundwater; however, because of its exposure to the surface. It is highly susceptibleto pollution throughanthropogenic activities. In addition to this, the construction of surface water harvesting structures for different purposes are costly and covers a larger area than groundwater points. Because of all these advantages the groundwater demand for domestic, irrigation, industrial, etc. increasing from year to year. In countries like Ethiopia, the demand for groundwater is enhanced because of fast population growth, urbanization and continuedeconomic development of the nation in general. Likewise, groundwater is the most common resource utilized for domestic water supply, agriculture, andlivestock in the present study area.

The common techniques of groundwater exploration using geophysical methods are expensive and time-consuming (Fenta et al., 2014; Fetter, 1994; Nsiah et al., 2018; Roscoe, 1990; Sener et al., 2005). These problems have forced people to use other technologies that can help investigate large areas in a short period of time with limited resources. These methods, including GIS and remote sensing, have been adapted to delineate groundwater potential zones. It is very easy and faster method for mapping groundwater potential zone in different geology conditions (Adji and Sejati, 2014; Nair et al., 2019; Siva et al., 2017). The RS and GIS approaches have been applied to delineate groundwater potential zones throughout the globe by various researchers (Agarwal et al., 2009; Al-Shabeeb-Shabeeb et al., 2018; Das et al., 2018; Fenta et al., 2014; Murmu et al., 2019; Pinto et al., 2017; Sar et al., 2015; Singh et al., 2019; Siva et al., 2017; Thapa et al., 2017; Yeh et al., 2016). The exploration for and locating groundwater potential using RS and GIS directly or indirectly depend on geology, geomorphology (landforms), slope, soil type, rainfall, landuse and drainage parameters (Murasingh et al., 2018; Thapa et al., 2017). Locating the groundwater potential zone is very essential for sustainable utilization of the resources. It supports planners, decision makers and policymakers to protect the groundwater recourse from any quantity and quality impacts. The analytic hierarchy process (AHP) approach is one of the most extensively used multi-criteria decision-making models (Arulbalaji et al., 2019; Murmu et al., 2019). Basically, AHP is considered as a simple, transparent, effective, and reliable system (Ishizaka and Labib, 2011; Machiwal et al., 2011), and hence can be used for delineating groundwater potential zones (Patra et al., 2018). In this study, the groundwater potential zones are delineated by RS, GIS and AHP techniques using geology, geomorphology (landforms), slope, soil type, lineament density, drainage density, rainfall, landuse/landcover, Normalized differences vegetation index (NDVI), and Topographic wetness index (TWI) parameters. The findings are validated with the specific yield of the existing boreholes and discharge amount of the springs located in the particular areas.The main objective of thisstudy is to map and delineategroundwater potential zones using the integrated approaches which support sustainable development, planning, and utilization with proper management of groundwater for irrigation and drinking purposes.

1.2. Study area

Golina river basin is located in North Wollo Administration, Amhara Regional State, and Northern Ethiopia. It is bounded between 540810 and 585122m East longitude and 1352908 and 1318433m North latitude (*Figure 1*). It has a total of 916.77 km^{2}areal coverage and an elevation variation from 1326 to 3970 m above mean sea level. The basin is southwestern part of the Danakil depression, the northwestern Ethiopian plateau, and the marginal valley. It is surrounded by Raya Valley from the North, from the South by the Alwuha basin, from the East by the Gudina basin and from the West by the Nile basin. It is drained by Golina, Hormat and Kelkel rivers which are merged together near the outlet and exit the basin through the Golina outlet in the eastern part. The Golina River is perennial while the other two are intermittent streams. The Golina river basin is characterized by semi-arid climate conditions. The spatial distribution of the annual mean maximum and annual mean minimum temperaturesof the basin varies from 18 – 30^{o}C and 5 – 15^{o}C,respectively. The spatial distribution of the annual mean precipitation of the basin ranges from 764 to 1092mm per year.

Groundwater is the main sourceof water for the community, even if they used the river in some places for irrigation. The local community uses groundwater from developed springs and hand-dug wells in the mountainous area whileboreholes are used in the lowland.

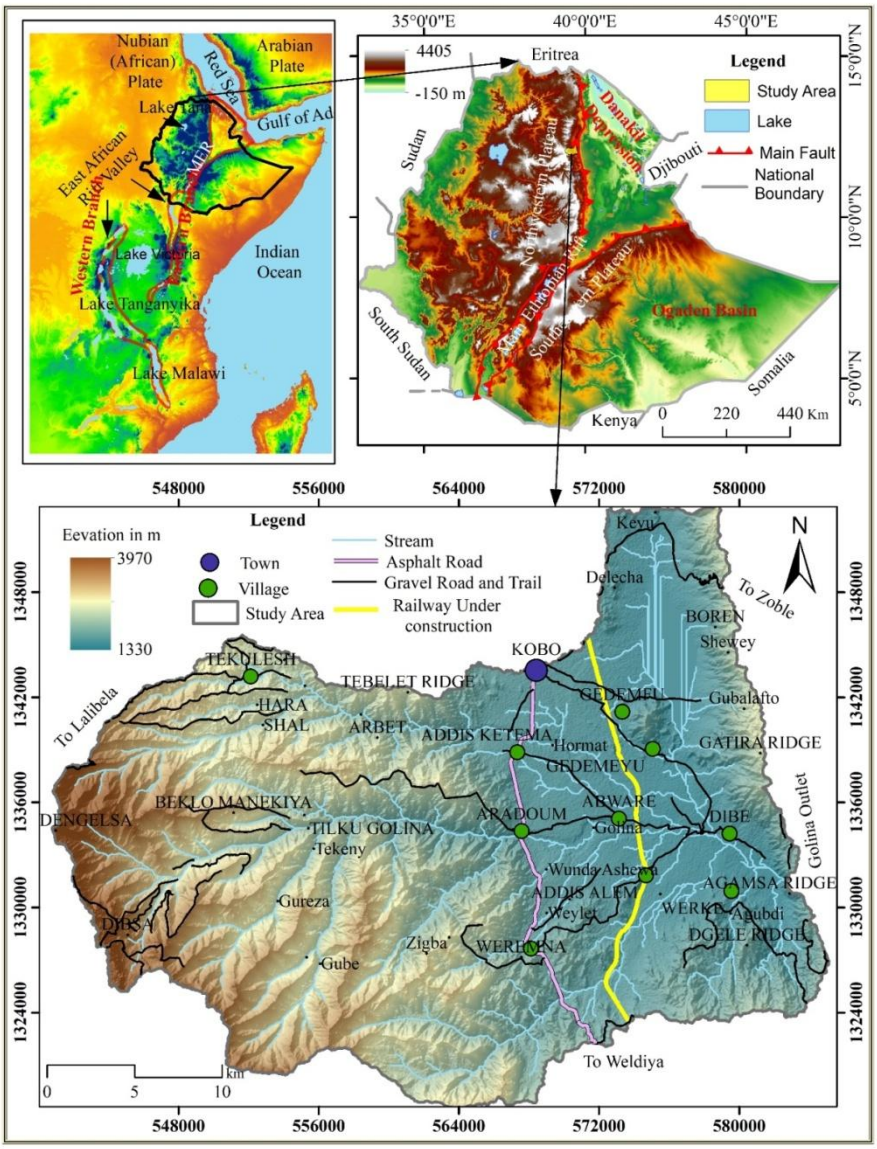

Figure 1: *Location map of the study area*

2. Methods

2.1. Thematic layers preparation

The groundwater potential of the area is delineated using ten thematic layer parameters namely geology, geomorphology (landforms), lineament density, drainage density, slope, soil, land use/cover, rainfall, normalized difference vegetation index (NDVI) and topographic wetness index (TWI). The boundary and the streams of the basin are extracted from DEM using the graphical user interface ArcSWAT in GIS software. The digital elevation model is downloaded from Advanced Land Observing Satellite (ALOS)Phased Array type L-band Synthetic Aperture Radar (PALSAR) with 12.5m spatial resolution (ASF DAAC, 2008). The geological map is prepared in the field. The main lithology and geological structures of the area are described in the field. The geomorphologiclandform of the areais prepared using SAGA GIS software. The landform is classified using TPI based landform classification. Lineaments are extracted from hills hadeusing PCI Geomatics software. The hillshade also prepared from the digital elevation model (DEM) of the basin using surface in the spatial analyst tool in GIS software. The drainage and lineament densities are developed from streams and lineaments using line density in spatial analysttool in GIS software. Landsat 8 OLI imagery was downloaded from the Earth Explorer, U.S. Geological Survey website *(www.earthexplorer.usgs.gov).* The NDVI is prepared from Landsat 8-OLI with 30m resolution using raster calculates in spatial analysis tool in GIS software. The slope of the area is prepared from DEM using surface in spatial analyst tool in ArcGIS 10.2 software. The daily rainfall of the study area is collected from 1992 to 2016 in 11stations from the Ethiopian National Meteorological Agency (ENMA). The stations used for the analysis Alamata, Chercher, Dilb, Kobo, Korem, Lalibela, Sanka, Sirinka, Waja, Robit, Muja, Woldia, and Zobel. Among these, Kobo and Robit are located within the boundary of the study area while Alamata, Chercher, Dilb, Korem, Lalibela, Sanka, Sirinka, Waja, Muja, Woldia, and Zobel are located outside of the basin. The mean annual rainfall isinterpolated using an inverse distance weighting (IDW) technique in GIS software. The TWI is calculated from the flow accumulation and slope of the basin using the raster calculator in Map algebra in GIS software. Land use/cover is developed from the Landsat 8_OLI using supervised image classification in ArcGIS 10.2 software. It is validated by comparing with sample training that is collected from the ground during the field visits and from Google earth. The soil map of the area is prepared from a raw data gathered by Metaferia contractor engineer (MCE) consult (2007) and data downloaded from Soil grid with 2.5 km resolution (for the area which is not covered by MCE consult). The groundwater point data are collected from different governmental and non-governmental organizations. The general flow chart of the methodology is given in Figure 2.

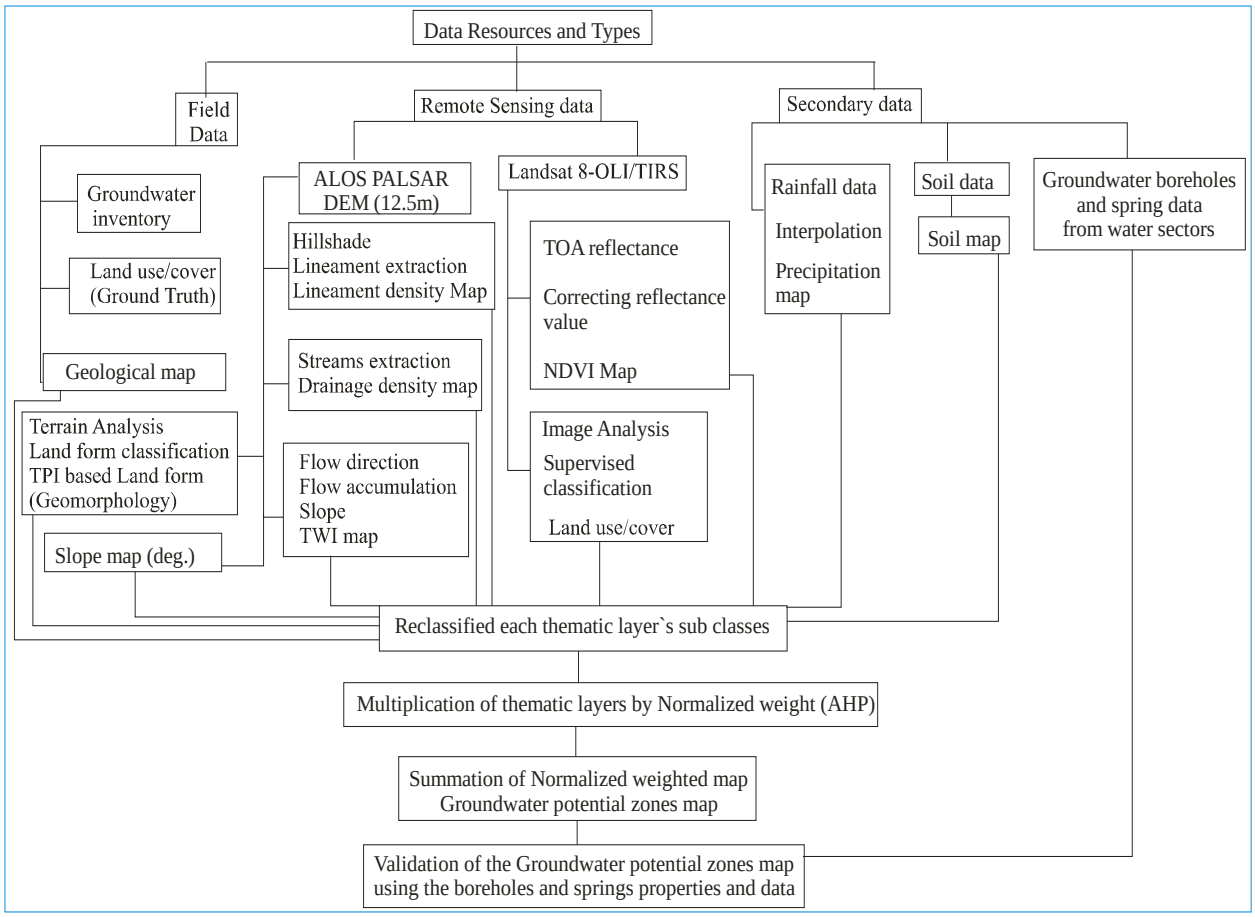

Figure 2: *Flow chart of the methodology*

2.2. Multi-criteria decision analysis using AHP

According to Arulbalaji et al. (2019), multi-criteria decision analysis using Analytical Hierarchical Process (AHP) is the most common GIS-based method for demarcating groundwater potential zones. The AHP method is used to generate and integrate all thematic layers based on their importance and influences for groundwater potential. In this study, a total of 10 thematic layers are used. These thematic layers are selected based on their importance for groundwater storage and transmissivity. The first procedure of this approach is to assign (Saaty, 2005, 1980) scales for pairwise comparison of the thematic layer's matrix. The two thematic layers which have equal importance for groundwater potential are assigned 1 but for the extreme importance of the pairs are given 9 (Table 1). The analytical hierarchical process (AHP) method is used for both the class of the layers and the thematic layers to identify their ranks and priority for the groundwater potential. Hence, the total weight (TW) in Table 3 is determined from the total scale weight divided by a total number of parameters for all thematic layers and classes of layers. Then, the normalized weight is derived from the assigned weight of a parameter feature class divided by the corresponding geometric mean (Kaliraj et al., 2014; Nair et al., 2019). The thematic layer with a higher normalized weight value shows a higher influence where as a lower value illustrates a less important on the groundwater potential zones (Magesh et al., 2012). The principal Eigenvalues of the parameters and class are derived from the total weight and normalized weight factors.

Table 1: *Saaty's Scale of Relative Importance (Saaty, 2005)*

Scale	Numerical rating	Reciprocal
Equal importance	1	1
Equal to moderate importance	2	1/2
Moderate importance	3	1/3
Moderate to strong importance	4	1/4
Strong importance	5	1/5
Strong to very strong importance	6	1/6
Very strong importance	7	1/7
Very strong to the extreme importance	8	1/8
Extreme importance	9	1/9

The λ_{max} values of the thematic layer and classes are computed from the largest Eigen values to check the decision consistency of the pair wise comparison as shown in the equation below. It is the summation of the product of total weight and normalized weight of the parameters in the matrix.

$$\lambda_{max} = \sum_{i=1}^{n} TW_i * NW_i \qquad \text{Eq. 1}$$

Where λ_{max} for the largest Eigen values, TW_i for the total weight and NWi for the Normalized weight of the thematic layers.

Saaty (1980) defines the consistency index, the measure of consistency, deviation or degree of variation of consistency and computed using the following formula (Eq.).

$$CI = \frac{\lambda max - n}{n-1} \qquad \text{Eq. 2}$$

Where CI denoted for consistency index, λ_{max} for the largest Eigen values and n is n^{th} number of thematic layers

He proposed to use the consistency index by comparing with the appropriate consistency index so-called Random consistency index (RI) which is given in *Table 2*.

Table 2: *Random consistency index (Saaty, 1980)*

n	1	2	3	4	5	6	7	8	9	10
RI	0	0	0.58	0.9	1.12	1.24	1.32	1.41	1.45	1.49

The comparison between the consistency index (CI) and random consistency index (RI) is called consistency ratio (CR) which is computed using the following equation:

$$CR = \frac{CI}{RI} \qquad \text{Eq. 3}$$

Where CR denoted for consistency ratio, CI for consistency index and RI for random consistency index According to Saaty (1980), the value of the Consistency Ratio should be smaller or equal to 0.1 to accept in the consistency, otherwise, it needs to revise the judgment.

Table 3: *shows the assigned weights, the total weights of the thematic layers and Normalized weights (CI = 0.11 and CR = 0.08)*

TL	GMLF	Geo	LD	SP	DD	SL	LUC	PPT	NDVI	TWI	NW
GMLF	1	2	3	2	2	3	4	5	6	7	0.22
Geo	1/2	1	2	3	4	5	6	7	7	7	0.22
LD	1/3	1/2	1	2	3	4	5	6	7	7	0.17
SP	1/2	1/3	1/2	1	2	3	4	5	6	3	0.12
DD	1/2	1/4	1/3	1/2	1	2	3	5	4	5	0.09
SL	1/3	1/5	1/4	1/3	1/2	1	2	3	5	4	0.07
LUC	1/4	1/6	1/5	1/4	1/3	1/2	1	0.5	2	3	0.04
PPT	1/5	1/7	1/6	1/5	1/5	1/3	2	1	2	3	0.04
NDVI	1/6	1/7	1/7	1/6	1/4	1/5	1/2	1/2	1	2	0.02
TWI	1/7	1/7	1/7	1/3	1/5	1/4	1/3	1/3	1/2	1	0.02
TW	3.93	4.88	7.74	9.78	13.48	19.28	27.83	33.33	40.5	42	1.00

Where: TL – Thematic Layers, GMLF – Geomorphologic Landform, Geo – Geology, LD – Lineament Density, SP – Slope, DD – Drainage Density, LUC – Land Use/Cover, PPT – Precipitation, NDVI – Normalized Difference Vegetation Index, TWI – Topographic Wetness Index, TW – Total Weight and NW – Normalized Weight.

2.3. Groundwater Potential calculation

The weight map of the thematic layer feature classes is prepared using ArcGIS to compute the groundwater potential zones of the study area using the following equation. The normalized weights of the themes multiplied by the normalized weights of the class are applied to evaluate the groundwater potential index using the raster calculator in ArcGIS 10.2 software.

$$GWPI = GM_w * GM_{wi} + Geo_w * Geo_{wi} + LD_w * LD_{wi} + SP_w * SP_{wi} + DD_w * DD_{wi} + SL_w * SL_{wi} + LULC_w * LULC_{wi} + PPT_w * PPT_{wi} + NDVI_w * NDVI_{wi} + TWI_w * TWI_{wi} \quad \text{Eq. 4}$$

Where: GWPI refers to groundwater potential index, GM for geomorphologic landform, Geo for geology, LD for lineament density, SP for slope, DD for drainage density, SL for soil texture, LULC for land use land cover, PPT for precipitation, NDVI for normalized difference vegetation index, TWI for Topographic wetness index, and the subscribes of w and wi are for the normalized weights of the themes and normalized weights of the feature class, respectively.

Table 4: *Class of thematic layers with normalized weights*

Thematic layer (w)	Classes	wi	Thematic layer (w)	Classes	wi
Geo (0.22)	CI = 0.082, CR = 0.062		SL (0.07)	CI = 0.046, CR = 0.035	
	Alluvial deposit	0.36		Sand	0.35
	Tarmaber formation	0.21		Sandy Loam	0.24
	Alaje formation	0.16		Sandy Clay	0.16
	Aiba formation	0.11		Loam	0.11
	Ashangi formation	0.10		Clay Loam	0.07
	Rhyolite	0.04		Silty Clay	0.05
	Granite	0.02		Clay	0.03

GM (0.22)	CI = 0.094, CR = 0.063	
	Plains	0.29
	Valley	0.21
	open slopes	0.15
	Upper slopes	0.11
	Mid slope Drainage	0.08
	Stream	0.06
	Upper Drainage	0.04
	Local Ridges	0.03
	Mid slope ridges	0.02
	High ridges	0.02
LI (0.17)	CI = 0.03, CR = 0.027	
	Very high (4.0-5.15)	0.42
	High (3.0-4.0)	0.26
	Medium (2.0-3.0)	0.18
	Low (1.0-2.0)	0.09
	very low (0.0-1.0)	0.05
SI (0.12)	CI = 0.046, CR = 0.041	
	Flat (0-8.0)	0.45
	Gentle slope (8.1-16)	0.29
	Medium slope (17.1-30.0)	0.15
	Steep slope (30.1-45)	0.07
	Very steep (45.1-78)	0.04
DD (0.09)	CI = 0.006, CR = 0.01	
	Low (<1)	0.54
	Medium (1 - 2)	0.30
	High (>2)	0.16

LUC (0.04)	CI = 0.085, CR = 0.064	
	Waterbody	0.42
	Agricultural land	0.21
	Glass land	0.14
	Forest land	0.09
	Shrub	0.07
	Bare land	0.04
	Residential	0.02
PPT (0.04)	CI = 0.022, CR = 0.020	
	1095.0-1025.0	0.42
	1025.1-960.0	0.26
	960.1-895.0	0.16
	895.1-825.0	0.10
	825.1-760.0	0.06
NDVI (0.02)	CI = 0.023, CR = 0.020	
	Very high (>0.50)	0.42
	High (0.30-0.50)	0.26
	Intermediate (0.10-0.30)	0.16
	Low (0-00-0.10)	0.10
	Very low (<0)	0.06
TWI (0.02)	CI = 0.024, CR = 0.021	
	Very low SM (-8) - (-2.5)	0.05
	Low SM (-2.6) - 4	0.10
	Medium SM (4.1) - (8)	0.15
	High SM (8.1) - (12)	0.26
	Very high SM (12.1) -(22)	0.44

3. Results and Discussions

3.1. Thematic layers preparation

3.1.1. Geology

The geology of the Golina river basin is part of the Tertiary flood basalts of the northwestern Ethiopian plateau which is formed in the Cenozoic era before 30Mya (Hofmann et al., 1997). The northwestern Ethiopian plateau volcanic rocks are classified by Blandford (1870) as a lower Ashangi group unconformity overlain by the Magdala group. Later, these volcanic formations are regrouped by Zanettin and Justin Visentin (1973) and Gregnanin and Piccirillo (1974) as Ashangi and Aiba basalts, Alaje Rhyolites, and Termaber basalts.

The North-East part of the study area is covered with flow banded rhyolite rock. This rock unit is characterized by greenish, fine-grained, slightly weathered, ridge forming, compacted and associated with ignimbrite, tuffs, and Ash. The rock is porphyritic and composed of phenocrysts of K-feldspar, quartz, and plagioclase. The rhyolite rock is in contact with Ashangi formation as a result of northeast-striking sinistral strike-slip fault. Granite occurs as a ridge and hill forming intrusive rocks in the central valley. The granite rock has pinkish and greyish in fresh color, yellowish weathered color, medium to coarse-grained. It consists of quartz, k-feldspar, and pyroxenes. The alluvial deposits are exposed in the graben formed by western and eastern ridges. These sediments contain gravels, sand, silt, and sediments. The flow direction of the sediments shows from the western ridge towards the eastern part

of the graben. The grain size of the sediments is coarse near the mountainous while it isfine-grained in the central part of the graben. The stratigraphy of the sediments indicates that there were a series of sedimentation cycles.

From a hydrogeological point of view, areas covered with the alluvial deposits are the main groundwaterpotential areas. Thus, most of the boreholes drilled for domestic and irrigation purposes are concentrated in the alluvial deposits. According to Kebede (2013), the basal sequence (Ashangi basalt) is low permeability and low productive aquifer than the upper sequences (Aiba-Termaber-Alaji formations) of the Ethiopian volcanic plateau. The ridge forming rhyolite and granite rocks are impervious and nonproductive formations in the study area. Therefore, the normalized weight of the geology is arranged from high in alluvial deposits to low in granite (Figure 3).

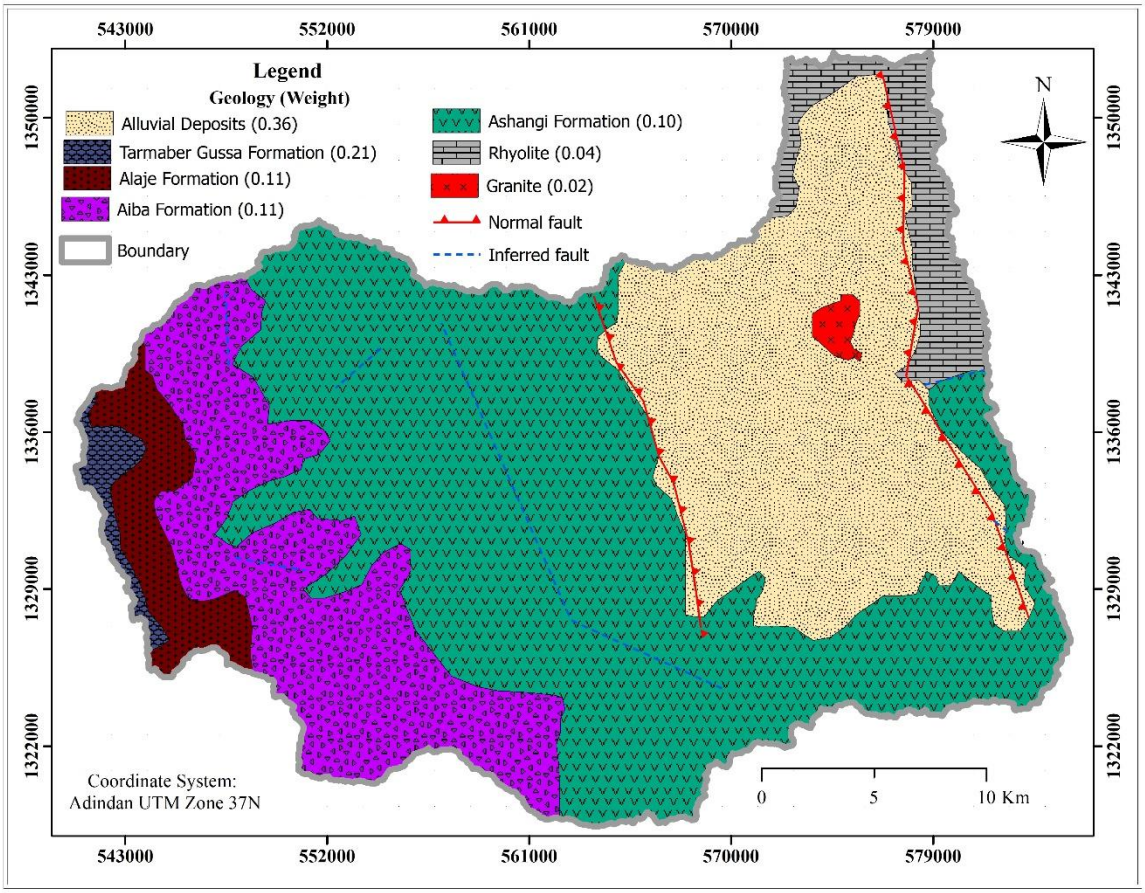

Figure 3: *Geological map.*

3.1.2 Geomorphologic Landform

The topographic terrain index-based landforms of the basin are prepared using SAGA GIS software from the digital elevation model(Conrad et al., 2015). The landform using topographic position index (TPI) is the difference between the elevation value of each cell in a digital elevation model (DEM) and the average elevation of the specified neighborhood around that cell (Weiss, 2001). Negative values (valley) mean the cell is lower than its surroundings while Positive values (ridge) mean it is higher. Accordingly, the area is classified into plain, valley, open slope, upper slope, midslope drainage, stream, upland drainage, local ridge, midslope ridge, and high ridges. The normalized weight value of plain and valley landforms are higher than the others for groundwater potential. But the ridge types are lower for groundwater potential as shown in (Figure 4). The graben part of the normal fault is dominated by plain and valley landform classes. The landforms of the western and eastern partsinclude all classes that indicate a rugged and rough topography.

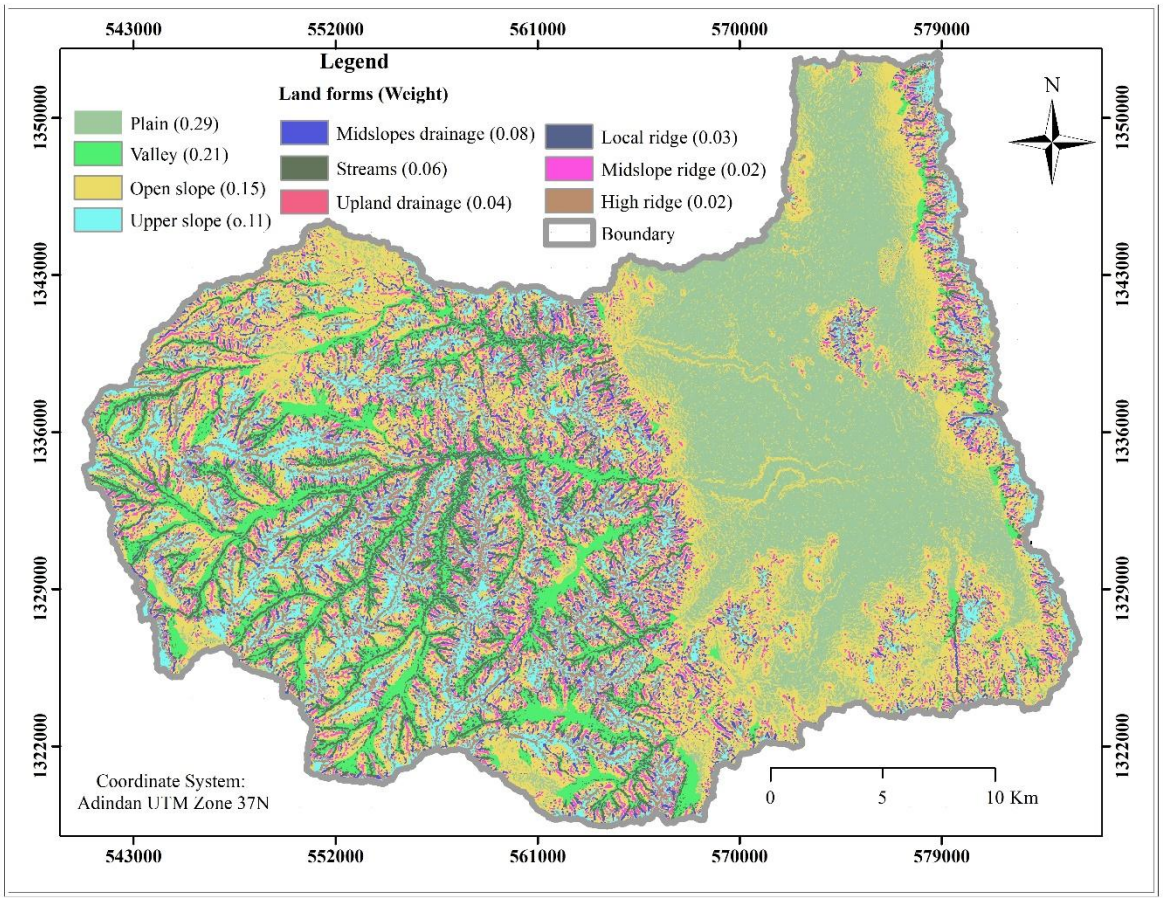

Figure 4: *Geomorphologic landforms map.*

3.1.3 Lineament and Lineament density

Lineament features are sources secondary porosity and permeability in hard rocks. They are very important for groundwater movement and storage. These lineaments are the linear features such as fault, joint, and fractures which serve as a container and conduit for groundwater storage and movement (Mukherjee et al., 2012; Obi Reddy et al., 2000). The groundwater movement and storage in hard rocks are controlled by lineaments and discontinuities because they are considered as subsurface secondary porosity. The intersection of various lineaments are areas where groundwater storage is possible keeping other parameters favorable for groundwater infiltration and storage. Lineament density map is important to reveal the groundwater recharge, flow, and development (Nag and Saha, 2014); (Murasingh et al., 2018). The lineament density is the ratio of the total lineament lengths and the unit area which expressed as Km per Km^2. The higher lineament density area have high groundwater potential especially when they are associated with the other parameters like landform and slope. The lineaments are extracted automatically from hillshade using line extraction in PCI Geomatics 2017 and the lineament density is also mapped using line density tool in ArcGIS 10.2. The dominant lineament orientation of the area is NE – SW as shows in the rose diagram (Figure 5).The lineament orientation has an impact on the groundwater flow direction of the area. The mountainous area has concentrated lineament and lineament density but sparsely dense in the lowland. The lineament density map is classified into five classes: less than 1 (very low), 1 – 2 (low), 2 – 3 (medium), 3 – 4 (high) and greater than 4 km/km^2 (very high) (Figure 5). The plain landform of the area has very low lineament density whereas very high is assigned in the high ridge and slope areas. Therefore, the weight for groundwater potential zone delineation is high in the high lineament density as shown in (Table 4).

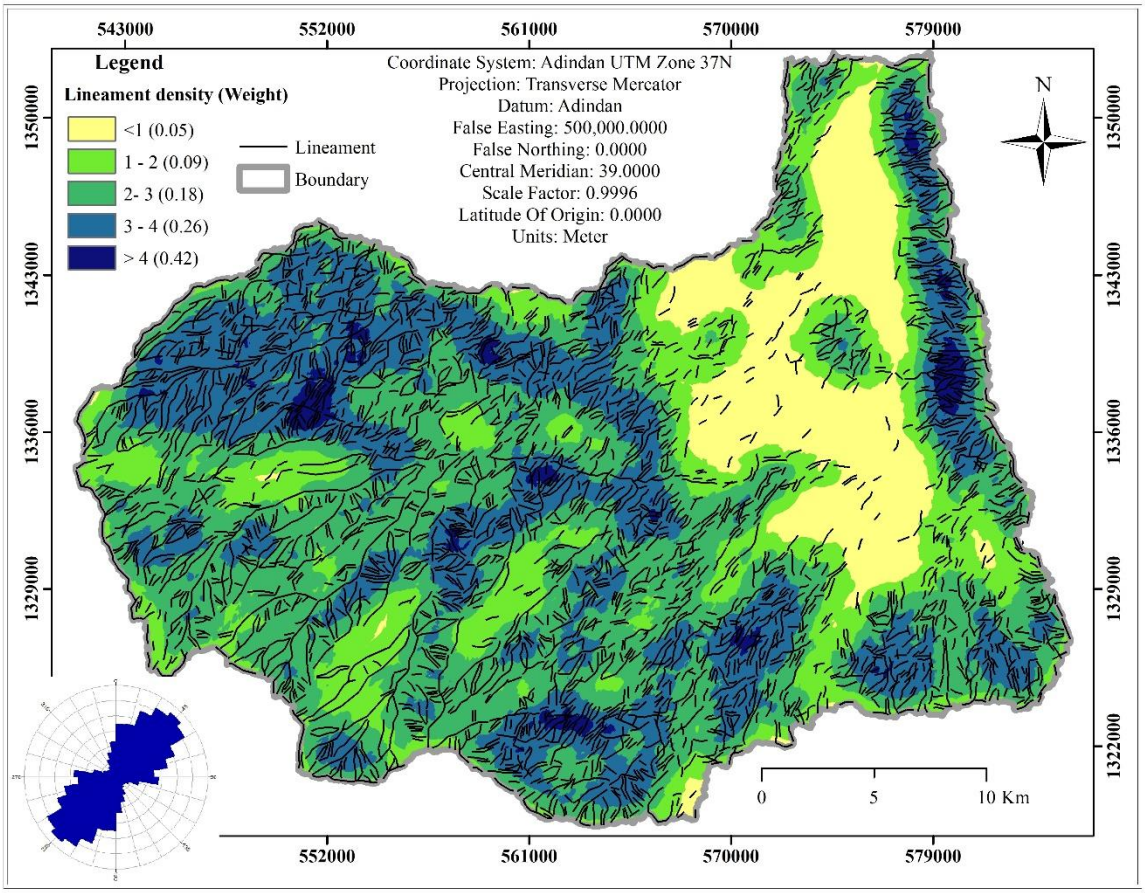

Figure 5: *Lineaments, Rose diagram, and lineament density.*

3.1.4 Slope

Slope is one of the factors controlling the processes of infiltration of surface water into the subsurface (Morbidelli et al., 2018).Slope has a vital role for the groundwater potential of the drainage basin because the infiltration rate increased with a decreasing slope angle. The study area is classified into five slope classes as below 7 degrees (flat plain), 7 to 15 degrees (gentle slope), 15 to 25 degrees (intermediate), 25 to 35 degrees (steep) and above 35 degrees (highly steep). The lower slope angle is very important for groundwater percolation whereas the highly steep is good for surface runoff. The rain that falls on the flat area with a small slope angle has a chance to join the groundwater table of the basin but on the highly steep area, it flows directly to the streams of the basin. Therefore, the western and eastern part of the basin is dominated by a variety of slope types which indicates a rugged topography and is susceptible to runoff rather than infiltration. The plains and valley landforms associated with a low slope is preferable for groundwater potential. So that the high weight is assigned for low slope (flat plain) whereas low weight is given for the very steep slopes due to their relative importance for groundwater potential (Figure 6).

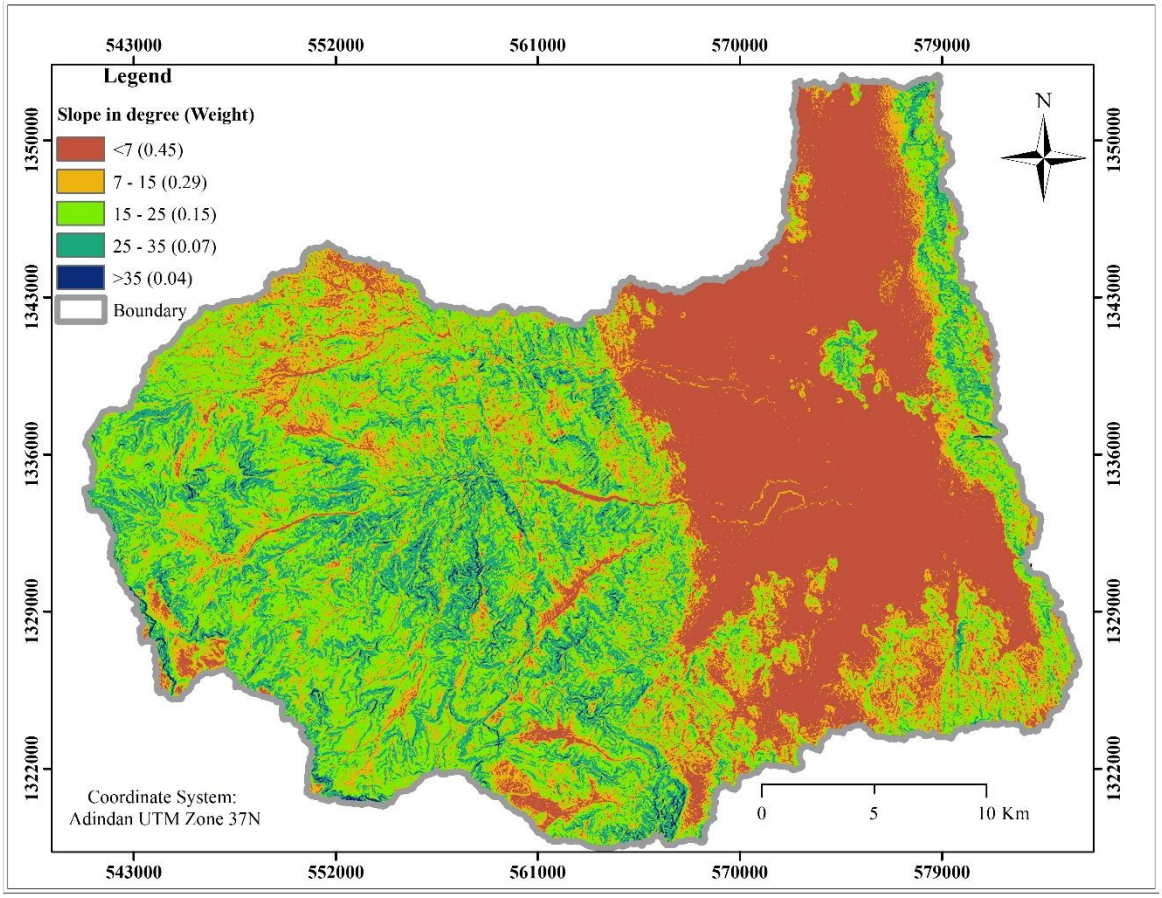

Figure 6: *Slope map.*

3.1.5 Drainage Pattern and Drainage Density

Drainage characteristics of a basin provided an indirect clue to the hydrogeological characteristics of the area and are useful for groundwater resources assessment (Singhal and Gupta, 1999). The main drainage characteristicsare drainage patterns and drainage density. The drainage pattern of the basin is systematically arranged as dendritic. This arrangement indicates the homogeneity of the lithology of the area which is dominated with a variety of basalt formations. Drainage density is the ratio of the total channel length of the streams within a basin to the area of the basin.

$$\mathrm{Dd} = \sum \frac{\mathrm{L}}{\mathrm{A}} \qquad \text{Eq. 5}$$

Where Dd is drainage density, L is the length of the streams, and A is an area of the basin.

According to the scale of the drainage map of the study area (Figure 7), the total length of the basin is 414.26 km within a total basin area of 916.77km^2 and therefore, the drainage density of the basin is 0.45 km/km^2.

The drainage density of a basin shows the nature of relief, climate, resistance to erosion and permeability of the rock materials (Singhal and Gupta, 1999). Moreover, the area with high drainage density indicates the high relief, low resistant to erosion, low permeability, high surface runoff, and very low groundwater recharge but the reverse nature is true for low drainage density area. The drainage density is high in the area where more streams joined together. The streams of the study area flow from the west to the east and are merged at the lower elevation near the outlet (Figure 7). An area with zero drainage density and without stream network is a potential for groundwater occurrence.

Therefore, the drainage density is divided into three main classes as less than 1 for low, 1 to 2 for medium and greater than 2 for high drainage density. Very low weight is given for high drainage density while the very high weight is given for the low drainage density of the area (Figure 7).

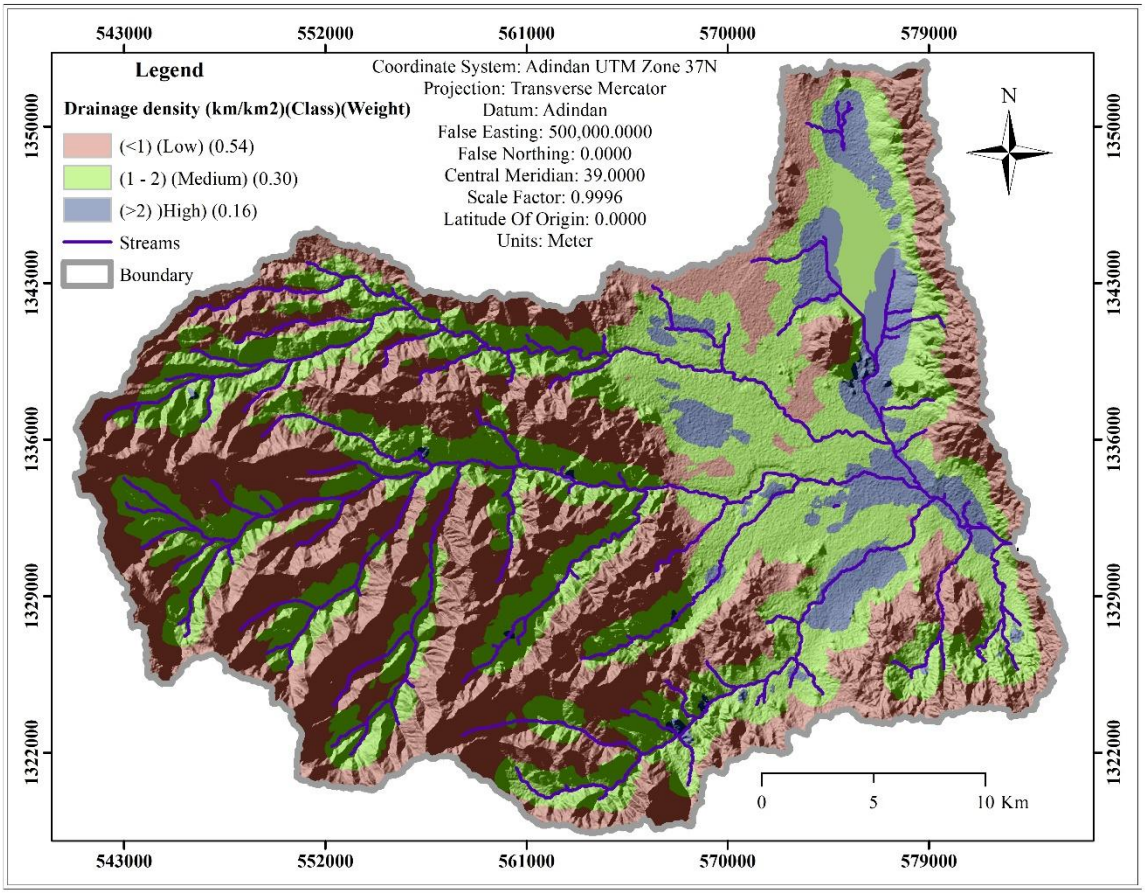

Figure 7: *Drainage density and streams.*

3.1.6 Soil Types

Groundwater recharge zones are places where the ground surface allows water infiltration and percolation through the soil (Chowdhury et al., 2009). The rate of water infiltration is directly depending on the grain size of the soils. Soil textures are a valuable thematic layer for groundwater potential and recharge assessment. Soil texture, the percentage of sand, silt, and clay, is an inherent factor affecting infiltration, percolation, and recharge. Water moves more quickly through large pores of sandy soil than through clayey soil. The sandy soils have a high infiltration rate than clayey soils. The coarse textures (e.g. Sand) is high permeability but the fine textures (e.g. Clay) show very low permeability. So that soil texture is strongly affecting the movement and storage of the groundwater. Based on the soil data derived from the literature, the study area has sand, sandy loam, sandy clay, loam, clay loam, silty clay, and clay soils. Accordingly, weights are given to the different soil classes in the area as indicated in Figure 8 (high for sand but low for clay).

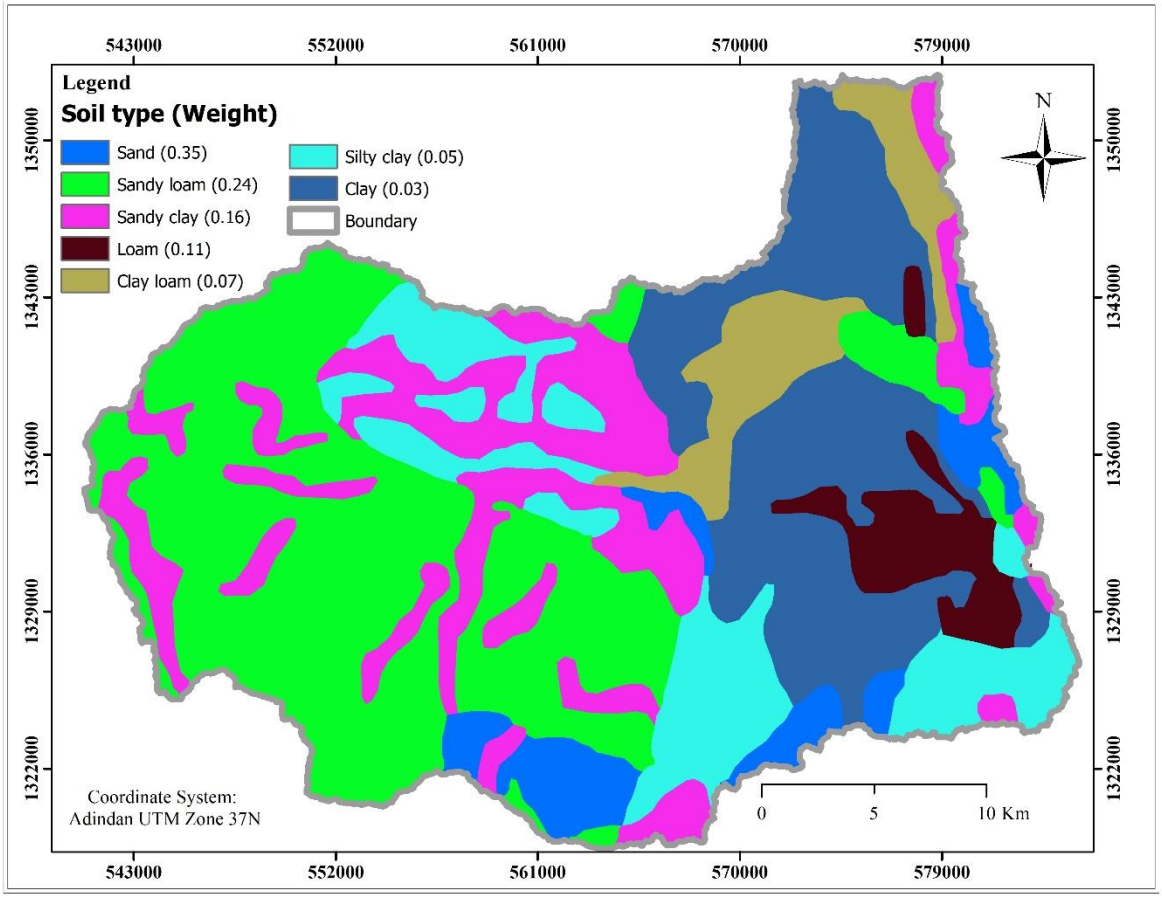

Figure 8: *Soil texture map.*

3.1.7 Land use/cover (LULC)

Understanding the effect of LULC on groundwater recharge and surface runoff is very interested in sustainable water resource management (Owuor et al., 2016). Moreover, accurate and reliable information about the present and future LULC will support in the management of resources (Murmu et al., 2019; Singh et al., 2018). The water addition from the unsaturated zone to the saturated zone of the water-bearing formation is affected by land use land cover. Even change in land use land cover will have an influence on the groundwater recharge, evaporation and surface runoff. The precipitation tends to infiltrate in the forest, vegetated and agricultural lands but tends to directly flow on the bare land and residential area as surface runoff. The land use land cover of the basin is categorized into a water body, cultivated land, natural forest, shrubland, bare land, and residential land and their groundwater recharge capacity decreases accordingly. So the highest weight is given to the water body and cultivated land and the lowest to residential and bare land (Figure 9).

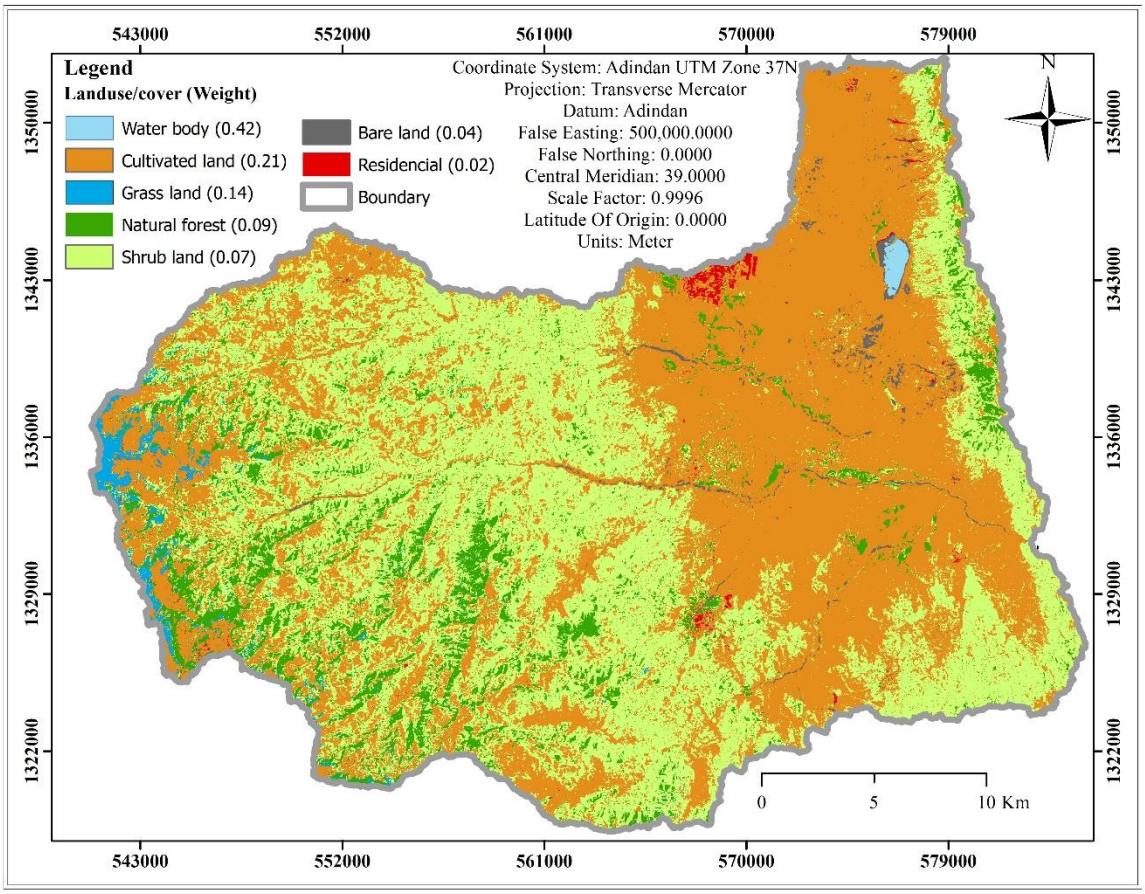

Figure 9: *Land use/cover map.*

3.1.8 Precipitation

Precipitation is the main source of groundwater recharge(Agarwal et al., 2009). The spatial distribution of precipitation of the study area is produced using the inverse distance weight interpolation method in ArcGIS software. The southwestern part of the basin receives high precipitation while the northeastern part receives low precipitation, relatively. The high-altitude area of the basin recorded high precipitation when compared with the low land altitude due to the orographic effect. As elevation decreases towards the east the precipitation also decreases. The mean annual precipitation of the study area ranges from 760 to 1095 mm/year with an average value of913 mm/year. The precipitation distribution in the basin can be grouped into five classes as 760 to 825, 825 to 895, 895 to 960, 960 to 1025 and 1025 to 1095 mm/year (Figure 10). The class with low precipitation is assigned low weight because of its less importance for groundwater potential. The class with high precipitation is assigned a higher weight. The area that received high precipitation has a chance to get more percolated water than the area that received low precipitation, keeping all other factors constant.

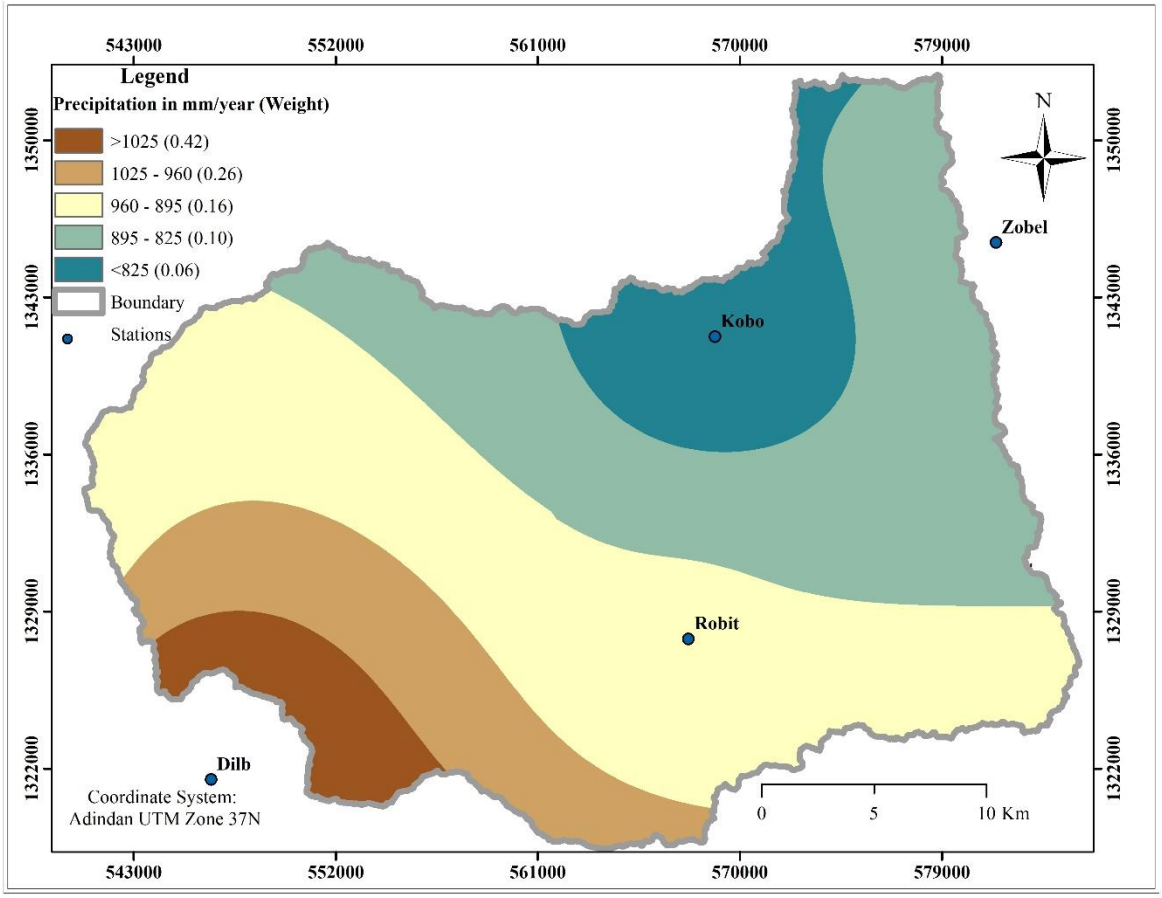

Figure 10: *Spatial distribution of precipitation*

3.1.9 Normalized Difference Vegetation Index (NDVI)

The normalized difference vegetation index is very essential for the delineation of groundwater potential zones (Sar et al., 2015). It is very important to assess the distribution of vegetation and the crop stage condition in the basin. The value with elevated vegetation area serves for infiltration rather than surface runoff because of the densely vegetated conditions. This is a method developed to easily distinguish between plants, water, and bare lands(Allestro and Parente, 2015).

The NDVI is counting vegetation by computing the difference between the near-infrared band and visible red band from Landsat 8 OLI using the following equation.

$$\mathrm{NDVI} = \frac{(\mathrm{NIR}-\mathrm{Red})}{(\mathrm{NIR}+\mathrm{Red})} \qquad \text{Eq. 8}$$

Where NDVI is normalized difference vegetation index, NIR is near-infrared (band 4) and Red is visible red (band 3) in Landsat 8 OLI.

Accordingly, the study area is reclassified into five NDVI classes as less than zero (very low vegetation coverage), 0 to 0.1 (low), 0.1 to 0.3 (intermediate), 0.3 to 0.5 (high) and greater than 0.5 (high vegetation coverage) (Figure 11). The area covered with high vegetation is assigned a high weight and the area covered with low vegetation is assigned low weight according to their importance for recharge (Table 4).

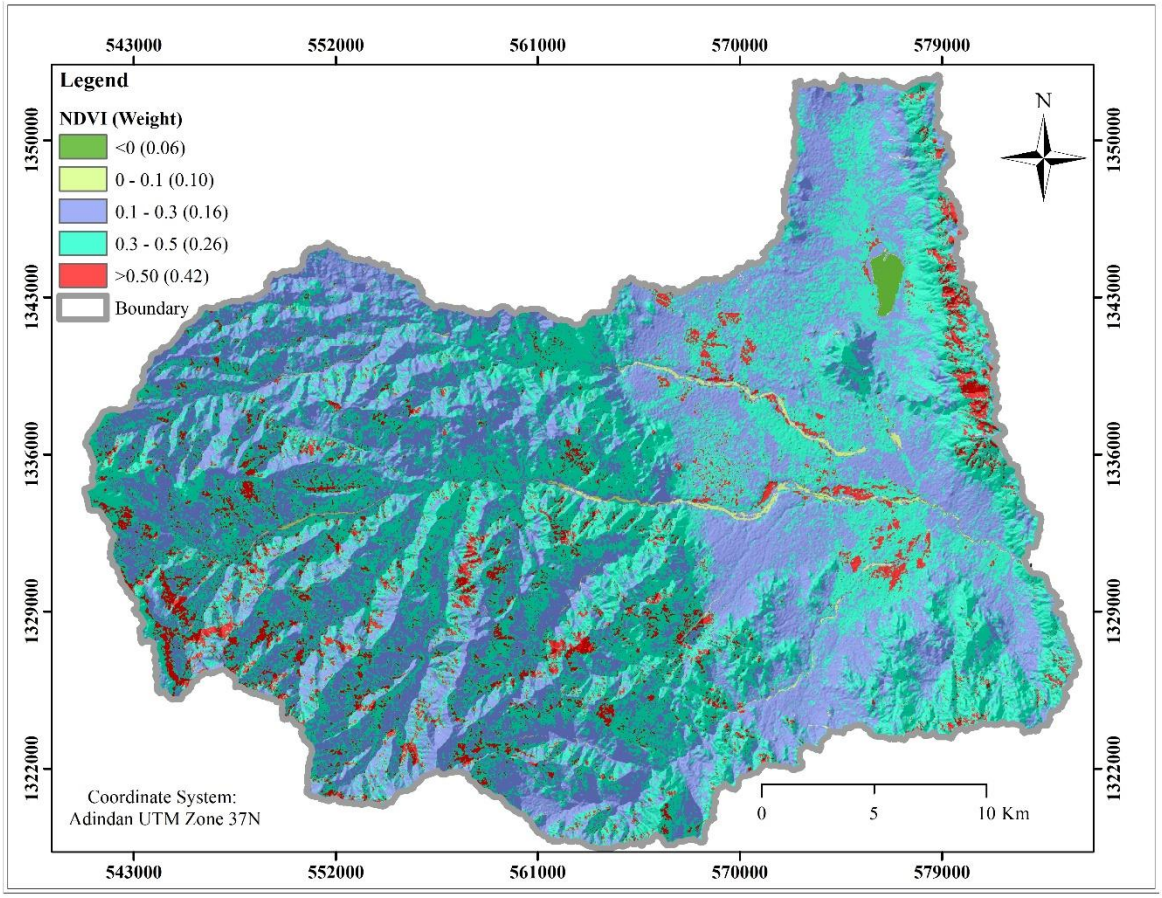

Figure 11: *Normalized difference vegetation index (NDVI) map.*

3.1.10 Topographic Wetness Index (TWI)

The topographic wetness index quantifies the tendency of soil water distribution, which is affected by topography (Beven and Kirkby, 1979; Raduła et al., 2018). It reflects the potential groundwater infiltration caused by the effects of topography (Arulbalaji et al., 2019; Mokarram et al., 2018). TWI is computed in SAGA GIS software using the following formula from DEM.

$$TWI = \ln\left(\frac{\alpha}{\tan\beta}\right) \qquad \text{Eq. 9}$$

Whereα is the upslope contributing area while β is the topographic gradient (slope). The upslope contributing area was estimated from the flow accumulation of the basin and the slope is in degree. The TWI value of the basin ranges from -8 to 22. These values are reclassified into five TWI classes from -8 to -2.5, -2.6 to 4, 4.1 to 8, 8.1 to 12 and 12.1 to 22 (Figure 12). The highest value indicates the presence of high soil moisture but the low value is soil without moisture or water. The highest class is assigned with high weight for groundwater potential and vice-versa. The lowland part of the area is found to be of high soil moisture area than the high lands. TWI indicates the soil moisture content and the groundwater storage are affected by the topography of the area. The water body and streams have the highest values of TWI.

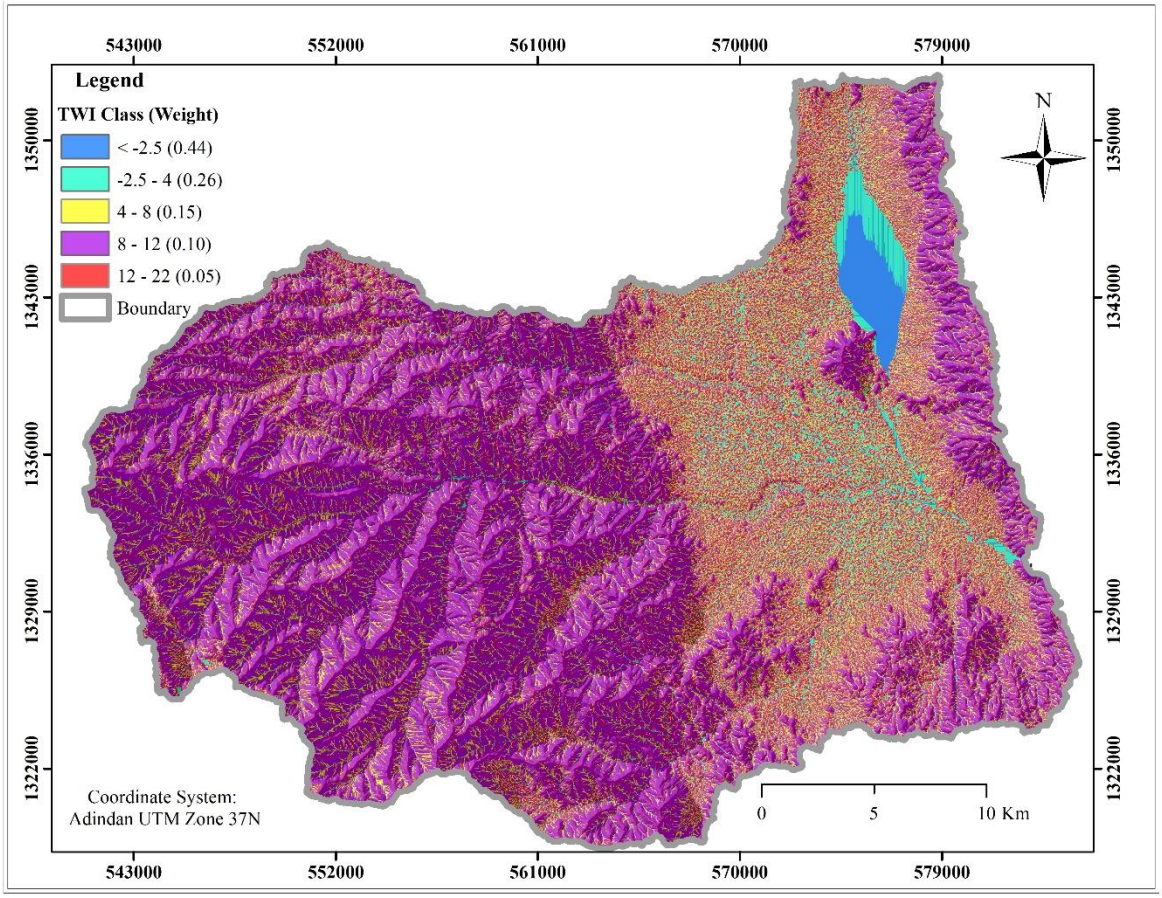

Figure 12: *Topographic wetness index (TWI) map.*

3.2 Groundwater Potential Zone and Validation

The resulting groundwater potential map of the study area indicated five discrete zones representing very good, good, moderate, poor and very poor groundwater potential areas (Figure 13). The total areal extent of the very good groundwater potential is162 km^2 (18%). Most of the very good groundwater potential is found in the eastern part of the study area which is an alluvial deposit, very low slope (flat), plain and valley geomorphologic landforms. Similarly, the area extent of good, moderate, poor and very poor are 221 km^2 (24%), 175 km^2 (19%), 265 km^2(29%) and 93 km^2 (10%), respectively (Table 5).

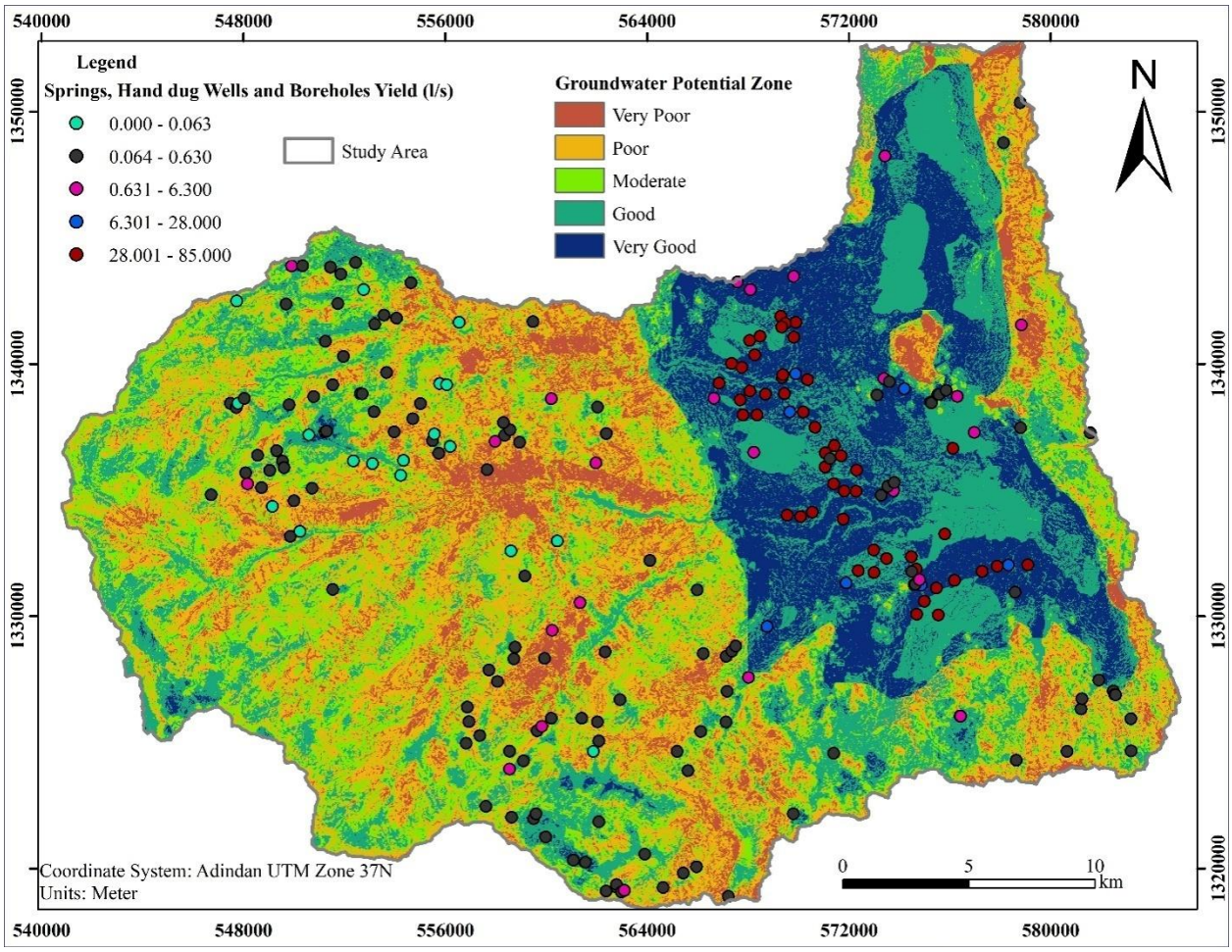

Figure 13: *Groundwater potential zones.*

The good and moderate groundwater potential zones are found in the alluvial deposits and Termaber formations, at the bottom of the ridges, in the intermountain valleys, near streams and around dense lineaments. The poor and very poor groundwater potential areas are mainly visible in Ashangi formation, granite, and rhyolite, ridges, sparsely lineament density and steep slope areas. The result shows that the central and western parts of the area are not suitable for groundwater potential.

Table 5: *Groundwater potential zones*

S.No.	Groundwater potential zone	Area (Km2)	% of the total area	No. of water points
1	Very good	162	18	74
2	Good	221	24	72
3	Moderate	175	19	48
4	Poor	265	29	59
5	Very poor	93	10	10

The groundwater potential map of the study area is validated with the existing groundwater borehole and springs yield. Most of the deep boreholes which serve for irrigation purposes are concentrated in the very good and good groundwater potential zones. The yields of the boreholes are greater than 28 l/s. The groundwater points (springs, hand-dug wells, and boreholes) of the area are classified based on their magnitude of yields into five groups as those with a yield less than 0.063, 0.063 to 0.63, 6.3 to 28 and greater than 28 l/s (Figure 13). The springs and hand-dug wells with very low yield are located in the very poor, poor and moderate groundwater potential. The low yield springs are mainly concentrated in the poor groundwater potential zone of the area. About 50 boreholes with a yield greater than 28 l/s are drilled in the area and 39 of them are concentrated in the very good

groundwater potential zone (Table 6). Only 10 springs are found on the very poor groundwater potential zone.

Table 6: *The number of springs, hand-dug wells, and boreholes in groundwater potential zones*

Groundwater Potential zones	< 0.063 l/s	0.063 - 0.63 l/s	0.63 – 6.3 l/s	6.3 – 28 l/s	> 28 l/s
Very Good	4	18	7	6	39
Good	12	37	11	1	11
Moderate	5	39	4	-	-
Poor	14	42	3	-	-
Very Poor	2	6	2	-	-

4. Conclusion and Recommendations

In this study, an attempt was made to delineate the different groundwater potential zones in the Golina River Basin where groundwater is used as a source of water for both supplementary and complementarydomestic and irrigation using the integratedmethods of the analytical hierarchy process (AHP), GIS and remote sensing. The result indicated that the groundwater potential of the area can be divided into five zones as very poor, poor, moderate, good and very good covering 10%, 29%, 19%, 24% and 18% of the total area of the basin, respectively. The results are validated using the existing springs, hand-dug wells, and borehole yields. Out of total50 boreholes, 11 and 39 boreholes serving for irrigation are drilled in the good and very good groundwater potential zones, respectively (Table 6), while the low yield springs and hand-dug wells are developed and drilled in the very poor, poor, moderate and in the good types of groundwater potential zones. This indicates that the AHP-GIS-Remote sensing integrated approach for groundwater potential identification gives an acceptable result. Hence, it is fair to conclude that this result can be used for the planning of new groundwater-based projects and expansion of the existing irrigation project in the basin.

Acknowledgment

The authors wish to thanks Samara University and Mekelle University for funding the research work. We would also like to extend our appreciation to the Ministry of Water, Irrigation, and Electricity of Ethiopia and the Water Resource Office of Kobo Wereda for providing us with the borehole and spring data.

References

Adji, T.N., Sejati, S.P., 2014. Identification of groundwater potential zones within an area with various geomorphological units by using several field parameters and a GIS approach in Kulon Progo Regency, Java, Indonesia. *Arab. J. Geosci.* 7, pp.161–172. https://doi.org/10.1007/s12517-012-0779-z

Agarwal, E., Agarwal, R., Section, G., 2009. Delineation of Groundwater Potential Zone : An AHP / ANP approach Abstract : pp.887–898.

Al-Shabeeb, A.A.R., Al-Adamat, R., Al-Fugara, A., Al-Amoush, H., AlAyyash, S., 2018. Delineating groundwater potential zones within the Azraq Basin of Central Jordan using multi-criteria GIS analysis. *Groundw. Sustain. Dev.* 7, pp.82–90. https://doi.org/10.1016/j.gsd.2018.03.011

Allestro, P.D., Parente, C., 2015. Gis application for ndvi calculation using landsat 8 oli images. *Int. J. Appl. Eng. Res.* 10, pp.42099–42102.

Arulbalaji, P., Padmalal, D., Sreelash, K., 2019. GIS and AHP Techniques Based Delineation of Groundwater Potential Zones: a case study from Southern Western Ghats, India. *Sci. Rep.* 9, pp.1–17. https://doi.org/10.1038/s41598-019-38567-x

ASF DAAC, 2008. ALOS PALSAR_Radiometric_Terrain_Corrected_high_res [WWW Document]. asf.alaska.edu. https://doi.org/DOI: 10.5067/Z97HFCNKR6VA

Beven, K.J., Kirkby, M.J., 1979. A physically based, variable contributing area model of basin hydrology. *Hydrol. Sci. Bull.* 24, pp.43–69. https://doi.org/10.1080/02626667909491834

Chowdhury, A., Jha, M.K., Chowdary, V.M., 2009. Delineation of groundwater recharge zones and identification of artificial recharge sites in West Medinipur district, West Bengal, using RS, GIS and MCDM techniques. *Environ. Earth Sci.* https://doi.org/10.1007/s12665-009-0110-9

Conrad, O., Bechtel, B., Bock, M., Dietrich, H., Fischer, E., Gerlitz, L., Wehberg, J., Wichmann, V., Böhner, J., 2015. System for Automated Geoscientific Analyses (SAGA) v. 2.1.4. *Geosci. Model Dev.* 8, pp.1991–2007. https://doi.org/10.5194/gmd-8-1991-2015

Das, B., Pal, S.C., Malik, S., Chakrabortty, R., 2018. Modeling groundwater potential zones of Puruliya district, West Bengal, India using remote sensing and GIS techniques. *Geol. Ecol. Landscapes* 00, pp.1–15. https://doi.org/10.1080/24749508.2018.1555740

Fenta, A.A., Kifle, A., Gebreyohannes, T., Hailu, G., 2014. Spatial analysis of groundwater potential using remote sensing and GIS-based multi-criteria evaluation in Raya Valley, northern Ethiopia. *Hydrogeol. J.* 23, pp.195–206. https://doi.org/10.1007/s10040-014-1198-x

Fetter, C.W., 1994. Applied hydrogeology. Upper Saddle River, N.J. : Prentice Hall.

Hofmann, C., Courtillot, V., Féraud, G., Rochette, P., Yirgu, G., Ketefo, E., Pik, R., 1997. Timing of the ethiopian flood basalt event and implications for plume birth and global change. *Nature.* https://doi.org/10.1038/39853

Ishizaka, A., Labib, A., 2011. Review of the main developments in the analytic hierarchy process. *Expert Syst. Appl.* https://doi.org/10.1016/j.eswa.2011.04.143

Kaliraj, S., Chandrasekar, N., Magesh, N.S., 2014. Identification of potential groundwater recharge zones in Vaigai upper basin, Tamil Nadu, using GIS-based analytical hierarchical process (AHP) technique. *Arab. J. Geosci.* 7, pp.1385–1401. https://doi.org/10.1007/s12517-013-0849-x

Kaur, T., Bhardwaj, R., Arora, S., 2017. Assessment of groundwater quality for drinking and irrigation purposes using hydrochemical studies in Malwa region, southwestern part of Punjab, India. *Appl. Water Sci.* 7, pp.3301–3316. https://doi.org/10.1007/s13201-016-0476-2

Kebede, S., 2013. Groundwater in Ethiopia: Features, Numbers and Opportinities. Springer Berlin Heidelberg, Verlag Berlin Heidelberg. https://doi.org/10.1007/978-3-642-30391-3

Kuisi, M. Al, Mashal, K., Al-Qinna, M., Hamad, A.A., Margana, A., 2014. Groundwater Vulnerability and Hazard Mapping in an Arid Region: Case Study, Amman-Zarqa Basin (AZB)-Jordan. *J. Water Resour. Prot.* 06, pp.297–318. https://doi.org/10.4236/jwarp.2014.64033

Machiwal, D., Jha, M.K., Mal, B.C., 2011. Assessment of Groundwater Potential in a Semi-Arid Region of India Using Remote Sensing, GIS and MCDM Techniques. *Water Resour. Manag.* 25, pp.1359–1386. https://doi.org/10.1007/s11269-010-9749-y

Magesh, N.S., Chandrasekar, N., Soundranayagam, J.P., 2012. Delineation of groundwater potential zones in Theni district, Tamil Nadu, using remote sensing, GIS and MIF techniques. *Geosci. Front.* https://doi.org/10.1016/j.gsf.2011.10.007

Mokarram, M., Shaygan, M., Sathyamoorthy, Di., 2018. Using DEM and GIS for evaluation of groundwater resources in relation to landforms in the Maharlou-Bakhtegan watershed, Fars province, *Iran. J. Water L. Dev.* 37, pp.121–126. https://doi.org/10.2478/jwld-2018-0031

Morbidelli, R., Saltalippi, C., Flammini, A., Govindaraju, R.S., 2018. Role of slope on infiltration: A review. *J. Hydrol.* https://doi.org/10.1016/j.jhydrol.2018.01.019

Mukherjee, P., Singh, C.K., Mukherjee, S., 2012. Delineation of Groundwater Potential Zones in Arid Region of India-A Remote Sensing and GIS Approach. *Water Resour. Manag.* https://doi.org/10.1007/s11269-012-0038-9

Murasingh, S., Jha, R., Adamala, S., 2018. Geospatial technique for delineation of groundwater potential zones in mine and dense forest area using weighted index overlay technique. *Groundw. Sustain. Dev.* 7, pp.387–399. https://doi.org/10.1016/j.gsd.2017.12.001

Murmu, P., Kumar, M., Lal, D., Sonker, I., Singh, S.K., 2019. Delineation of groundwater potential zones using geospatial techniques and analytical hierarchy process in Dumka district, Jharkhand, India. *Groundw. Sustain. Dev.* 9, p.100239. https://doi.org/10.1016/j.gsd.2019.100239

Nag, S.K., Saha, S., 2014. Integration of GIS and Remote Sensing in Groundwater Investigations: A Case Study in Gangajalghati Block, Bankura District, West Bengal, India. *Arab. J. Sci. Eng.* https://doi.org/10.1007/s13369-014-1098-3

Nair, N.C., Srinivas, Y., Magesh, N.S., Kaliraj, S., 2019. Assessment of groundwater potential zones in Chittar basin, Southern India using GIS based AHP technique. *Remote Sens. Appl. Soc. Environ.* 15, p.100248. https://doi.org/10.1016/j.rsase.2019.100248

Nsiah, E., Appiah-Adjei, E.K., Adjei, K.A., 2018. Hydrogeological delineation of groundwater potential zones in the Nabogo basin, Ghana. *J. African Earth Sci.* 143, pp.1–9. https://doi.org/10.1016/j.jafrearsci.2018.03.016

Obi Reddy, G.P., Chandra Mouli, K., Srivastav, S.K., Srinivas, C. V., Maji, A.K., 2000. Evaluation of ground water potential zones using remote sensing data - a case study of Gaimukh watershed, Bhandara district, Maharashtra. *J. Indian Soc. Remote Sens.* https://doi.org/10.1007/BF02991858

Owuor, S.O., Butterbach-Bahl, K., Guzha, A.C., Rufino, M.C., Pelster, D.E., Díaz-Pinés, E., Breuer, L., 2016. Groundwater recharge rates and surface runoff response to land use and land cover changes in semi-arid environments. *Ecol. Process.* 5. https://doi.org/10.1186/s13717-016-0060-6

Patra, S., Mishra, P., Mahapatra, S.C., 2018. Delineation of groundwater potential zone for sustainable development: A case study from Ganga Alluvial Plain covering Hooghly district of India using remote sensing, geographic information system and analytic hierarchy process. *J. Clean. Prod.* 172, pp.2485–2502. https://doi.org/10.1016/j.jclepro.2017.11.161

Pinto, D., Shrestha, S., Babel, M.S., Ninsawat, S., 2017. Delineation of groundwater potential zones in the Comoro watershed, Timor Leste using GIS, remote sensing and analytic hierarchy process (AHP) technique. *Appl. Water Sci.* 7, pp.503–519. https://doi.org/10.1007/s13201-015-0270-6

Raduła, M.W., Szymura, T.H., Szymura, M., 2018. Topographic wetness index explains soil moisture better than bioindication with Ellenberg's indicator values. *Ecol. Indic.* 85, pp.172–179. https://doi.org/10.1016/j.ecolind.2017.10.011

Roscoe, M.C., 1990. Handbook of Groundwater Developement, 1st edn. ed. Wiley-Interscience.

Saaty, T.L., 2005. Analytic Hierarchy Process. Hoboken, NJ Wiley Online Libr. Encycl. Biostat. https://doi.org/10.1002/0470011815.b2a4a002

Saaty, T.L., 1980. The Analytic Hierarchy Process, Decision Analysis. https://doi.org/10.3414/ME10-01-0028

Sar, N., Khan, A., Chatterjee, S., Das, A., 2015. Hydrologic delineation of ground water potential zones using geospatial technique for Keleghai river basin, India. Model. *Earth Syst. Environ*. 1, pp.1–15. https://doi.org/10.1007/s40808-015-0024-3

Sener, E., Davraz, A., Ozcelik, M., 2005. An integration of GIS and remote sensing in groundwater investigations: A case study in Burdur, Turkey. *Hydrogeol. J.* 13, pp.826–834. https://doi.org/10.1007/s10040-004-0378-5

Singh, S.K., Laari, P.B., Mustak, S., Srivastava, P.K., Szabó, S., 2018. Modelling of land use land cover change using earth observation data-sets of Tons River Basin, Madhya Pradesh, India. *Geocarto Int.* https://doi.org/10.1080/10106049.2017.1343390

Singh, S.K., Zeddies, M., Shankar, U., Griffiths, G.A., 2019. Potential groundwater recharge zones within New Zealand. *Geosci. Front.* 10, pp.1065–1072. https://doi.org/10.1016/j.gsf.2018.05.018

Singhal, B.B.S., Gupta, R.P., 1999. Applied hydrogeology of Fractured rocks, 2nd edn. ed. Springer Science+Business, London New York. https://doi.org/10.1007/978-90-481-8799-7

Siva, G., Nasir, N., Selvakumar, R., 2017. Delineation of Groundwater Potential Zone in Sengipatti for Thanjavur District using Analytical Hierarchy Process. *IOP Conf. Ser. Earth Environ. Sci*. 80. https://doi.org/10.1088/1755-1315/80/1/012063

Taylor, R.G., Scanlon, B., Döll, P., Rodell, M., Van Beek, R., Wada, Y., Longuevergne, L., Leblanc, M., Famiglietti, J.S., Edmunds, M., Konikow, L., Green, T.R., Chen, J., Taniguchi, M., Bierkens, M.F.P., Macdonald, A., Fan, Y., Maxwell, R.M., Yechieli, Y., Gurdak, J.J., Allen, D.M., Shamsudduha, M., Hiscock, K., Yeh, P.J.F., Holman, I., Treidel, H., 2013. Ground water and climate change. *Nat. Clim. Chang.* 3, pp.322–329. https://doi.org/10.1038/nclimate1744

Thapa, R., Gupta, S., Guin, S., Kaur, H., 2017. Assessment of groundwater potential zones using multi-influencing factor (MIF) and GIS: a case study from Birbhum district, West Bengal. *Appl. Water Sci.* 7, pp.4117–4131. https://doi.org/10.1007/s13201-017-0571-z

Weiss, a, 2001. Topographic position and landforms analysis. Poster Present. ESRI User Conf. San Diego, CA. https://doi.org/http://www.jennessent.com/downloads/TPI-poster-TNC_18x22.pdf

Yeh, H.F., Cheng, Y.S., Lin, H.I., Lee, C.H., 2016. Mapping groundwater recharge potential zone using a GIS approach in Hualian River, Taiwan. Sustain. *Environ. Res.* 26, pp.33–43. https://doi.org/10.1016/j.serj.2015.09.005